This is a repository copy of *A Dynamic Predictive Traffic Signal Control Framework in a Cross-Sectional Vehicle Infrastructure Integration Environment*.

White Rose Research Online URL for this paper:
http://eprints.whiterose.ac.uk/145891/

Version: Accepted Version

A Dynamic Predictive Traffic Signal Control Framework in a Cross-Sectional Vehicle Infrastructure Integration Environment

Zhihong Yao, Luou Shen, Ronghui Liu, Yangsheng Jiang and Xiaoguang Yang

Abstract—**With the development of modern wireless communication technology, especially the vehicle infrastructure integration (VII) technology, vehicles' information such as identification, location, and speed can be readily obtained at upstream cross-section. This information can be used to support traffic signal timing optimization in real time. A dynamic predictive traffic signal control framework for isolated intersections is proposed in a cross-sectional VII environment, which has the ability to predict vehicle arrivals and use which to optimize traffic signals. The proposed dynamic predictive control framework includes a dynamic platoon dispersion model (DPDM) which uses the vehicles' speed data from cross-sectional VII environment, as opposed to traditional vehicle passing/existing data, to predict the arriving flow distribution at the downstream stop-line. Then, a dynamic programming algorithm based on the exhaustive optimization of phases (EOP) is proposed working in rolling optimization (RO) scheme with a 2 seconds time horizon. The signal timings are continuously optimized by regarding the minimization of intersection delay as the optimization objective, and setting the green time duration of each phase as a constraint. In the end, the proposed dynamic predictive control framework is tested in a simulated cross-sectional VII environment and carried out a case study based on a real road network. The results show that the proposed framework can reduce the average delay and queue length by up to 33% and 35% respectively compared to traditional full-actuated control.**

Index Terms—**Dynamic Predictive Control; Cross-Sectional Vehicle Infrastructure Integration; Dynamic Platoon Dispersion Model; Exhaustive Optimization of Phases; Rolling Optimization.**

I. INTRODUCTION

WITH the increase of automobiles in cities around the world, the consequent traffic congestion causes great social and economic costs. Traffic signal control plays an important role in relieving traffic

Z. Yao, L. Shen (*corresponding author*) and Y. Jiang are with School of Transportation and Logistics, Southwest Jiaotong University, National Engineering Laboratory of Integrated Transportation Big Data Application Technology, Sichuan 610031, China (e-mail: zhyao@my.swjtu.edu.cn, luoushen@home.swjtu.edu.cn, jiangyangsheng@swjtu.cn)

R. Liu is with Institute for Transport Studies, University of Leeds, Leeds LS2 9JT, UK (e-mail: R.Liu@its.leeds.ac.uk)

X. Yang is with Department of Traffic Engineering, Tongji University, Shanghai 201804, China (yangxg@tongji.edu.cn).

congestion. Traffic signal control theory has been established for over a century and a half, starting from the pioneering work of Webster [1]. Since then, research and development in traffic signal controls have experienced three levels of control methods: fixed-time control, actuated control, and responsive control.

Fixed-time control is based on historically collected traffic counts data and assumes traffic demand to be constant. Actuated control uses preset rules to dynamically adapt signal timing based on detected vehicle's passing/existing data. Responsive control used models to optimize the signal timing by analyzing detected traffic data in real time, in order to improve the performance and maximize the usage of intersection capacity [2-4]. There are a few widely used responsive traffic control systems in the world: SCATS [5] developed in Australia, SCOOT [6] developed in British, RODYN [7] and CRONOS [8] developed in France, UTOPIA [9] developed in Italy, and OPAC [10] and RHODES [11-12] developed in USA.

Most of these existing control systems rely on traffic data from the conventional loop-detectors or video cameras which mainly collect the vehicle passing/existing data. While, dual-loop detectors can collect vehicles' speed data, but there are not required for actuated or responsive control. Therefore, vehicles' speed data is not detected in the field for traditional traffic signal control. Recently, the development of electronic and communication technology [13], especially the Vehicle Infrastructure Integration (VII) technique, has enabled the information exchange between vehicles and infrastructure through wireless communication by installing onboard units (OBUs) and roadside units (RSUs). OBU and RSU can communicate with each other through Dedicated Short Range Communications (DSRC) technology. In a VII environment, except for the traditional traffic data, other data such as an individual vehicle's ID, speed and even acceleration et al can be directly collected [14].

In this paper, a special type of VII environment is developed. In a cross-sectional VII environment, RSUs are installed at specific roadside cross-section(s). This cross-sectional VII environment is much easier to implement compared to floating VII environment. This is because that on the one hand its communication is only needed at a limited number of locations. On the other hand, the positioning is not required since the location of the cross-section is already known. The floating VII environment performs communication continuously (actually in a very small period), and needs an additional channel for positioning [14]. In China, the VII environment, especially the cross-sectional VII environment is developing very fast in recent years. For example, the city of Chongqing has installed Radio Frequency Identification (RFID) detection roadside units (RSUs) at more than 900 cross-sections, and electronic license plates have been mandatorily installed for all local vehicles.

In a cross-sectional VII environment, RSUs are normally installed at road sections either on overhead gantries or under road surfaces. When vehicles pass the location, their IDs and speeds are transmitted to RSUs. In this paper, the real-time speed data collected in the upstream cross-sectional VII environment is used. Then, a dynamic platoon dispersion model [15] is developed to predict the arrival distribution at the downstream stop-line. The predicted arrival distributions can be used for signal timing optimization in real time. A dynamic programming (DP) algorithm called exhaustive optimization of phases (EOP) is proposed which includes the constraints of both minimum/maximum green times of each phase and considers the non-integer stage (or phase group) solutions by upgrading from the controlled optimization of phases (COP) [11] algorithm. Moreover, the proposed algorithm presented in this paper applies a rolling optimization (RO) scheme based on dynamic traffic arrival prediction in a cross-sectional VII environment.

The rest of paper is organized as follows: in the second section, a literature review of VII technology and signal control methods is presented; in the third section, the dynamic predictive control framework is presented; in the fourth section, a microsimulation environment is constructed based on a real road network, and the proposed algorithm is tested using simulation data; last but not least, conclusions and

future works are discussed.

II. LITERATURE REVIEW

VII technology is gaining increasing attention since vehicle' ID, speeds, and locations become available through the communication between OBUs and RSUs. In USA, the Federal Highway Administration (FHWA) supported University of Arizona to develop the "Next-Generation Smart Traffic Signals" [16], which is a VII technology based responsive signal control system: RHODESNG with IntelliDriveSM. Meanwhile, Virginia University [17] started the project of "IntelliDriveSM Traffic Signal Control Algorithms", which aimed at developing traffic control strategies for relieving congestion by monitoring traffic queues using VII technology.

Different from loop detector data, VII environment provide more information of the vehicle states, such as ID, speed and acceleration et al. By utilizing these data, traffic control decisions can be made to be more dynamically responsive to real-time traffic conditions. There have been several studies utilizing VII data for signal control. Priemer and Friedrich [14] first proposed the concept of applying VII technology to traffic signal control. They assume that vehicle' ID, locations, speeds, and time stamps are collected through wireless communication in a range of 300 m around the intersection. A dynamic programming algorithm is demonstrated to optimize signal timing using 5 secs as an optimization time step within a 20 secs prediction time horizon. Goodall et al. [18] proposed a predictive microscopic simulation algorithm (PMSA) for signal control. The algorithm assumes data is available in connected vehicle environment including position, headway, and speed. Then it utilizes a microscopic simulation model to predict future traffic conditions. A rolling horizon strategy of 15 secs was chosen to optimize either delay only or a combination of delay, stops, and decelerations. Goodall [19] considered several market proportions of connected vehicles (penetration rates) and the states of the unequipped vehicle were estimated based on the states of equipped vehicle. However, the algorithm cannot be applied in real-time due to the computational requirements of the parallel simulation to predict the future traffic conditions, especially for application to a big network.

He et al. [20] proposed a traffic signal control framework for multi-modes in a network of traffic signals under VII environment named PAMSCOD. A headway-based platoon recognition algorithm was developed to identify pseudo-platoons in the network. A mixed-integer linear programming (MILP) problem was solved to find the optimal signal plan based on current traffic conditions, controller status, platoon data, and priority requests. Simulation-based on a VISSIM model of two modes: transit and passenger cars, showed that PAMSCO can reduce delay for both under-saturated and oversaturated conditions. The results suggest that a 40% penetration rate was critical for effectively applying the algorithm. One limitation of PAMSCOD is that the computational requirements increase significantly with increasing traffic demand, since the number of decision variables is proportional to the traffic demand, and as such a real-time solution is not currently possible. Under the same VII framework, He et al. [21] integrated multi-modal priority control for emergency vehicles, transit buses, commercial trucks, and pedestrians, with the consideration of coordination and vehicle actuation. The signal coordination was treated as a virtual priority request in the formulation. However, utilizations of traditional vehicle actuation logic within the priority control framework may not be optimal for non-priority vehicles. Mckenney and White [22] investigated the microsimulation method to predict the traffic flow evolution using vehicles' location and speed data collected by VII technology, and optimized signal plans with the predicted traffic flow. Ahmane et al. [23] proposed a new approach for controlling the traffic at isolated intersections. They assumed that all vehicles are equipped with on-board units that allow them to

wirelessly negotiate the "right of way" according to their relative positions to the intersection. Lee et al. [24] studied a cumulative travel-time responsive real-time signal control method in a VII environment. The algorithm applied a Kalman Filter to estimate cumulative travel time under a low market penetration rate. The phasing with the highest combined travel time was set to be the next phase. The paper stated that at least 30% market penetration rate is required [20, 24].

Sen and Head [11] studied the signal control method for isolated intersection with traffic prediction based on detector data from the upstream intersection and developed the COP algorithm to optimize signal timing. The input traffic data to COP is predicted from detected traffic passing data at the upstream intersection by assuming vehicles traveling at constant speed. The COP applies both forward and backward recursions to search for the best timing plan within the prediction time horizon. Feng et al. [25] applied the COP algorithm with hypothetic data in a connected vehicle environment. However, there are restrictions in the COP algorithm: first, it did not consider the max green time. Therefore, more complications are faced in our study since the lower level of the model enumerates all cases for phase allocation. Second, it only considered integer stage solutions, that is, given a prediction time horizon, the algorithm could only find an optimal integer stage solution such as one, two, three, four or five stages within the prediction time horizon, which might not be the optimal solution.

This study is aimed at developing a dynamic predictive traffic signal control framework. Compared to previous studies, there are basically three aspects of improvements: DPDM for flow arriving prediction which using statistical distribution for speed data collected at upstream cross-section and dynamically updated within a certain time window; a DP algorithm of EOP for exhaustively optimizing timing plans which considers both the minimum and maximum green times of each phase, and allows non-integer stage within the prediction time horizon; and a RO scheme for adapting to real-time changes in traffic flows which applies for both the traffic prediction and signal timing optimization in a rolling time step of 2 secs.

III. FRAMEWORK OF DYNAMIC PREDICTIVE CONTROL SYSTEM

In this section, we present a dynamic predictive control framework for responsive signal control in a cross-sectional VII environment. The proposed EOP algorithm optimizes the signal phase durations based on predicted vehicle arrivals predicted by DPDM and updates following a 2 secs RO scheme, which belongs to the responsive traffic signal control category.

A. Signal timing optimization

Here, a typical 4-approach intersection signal control is studied which has 8 phases and 4 signal timing stages (or called phase groups) as shown in Fig. 1.
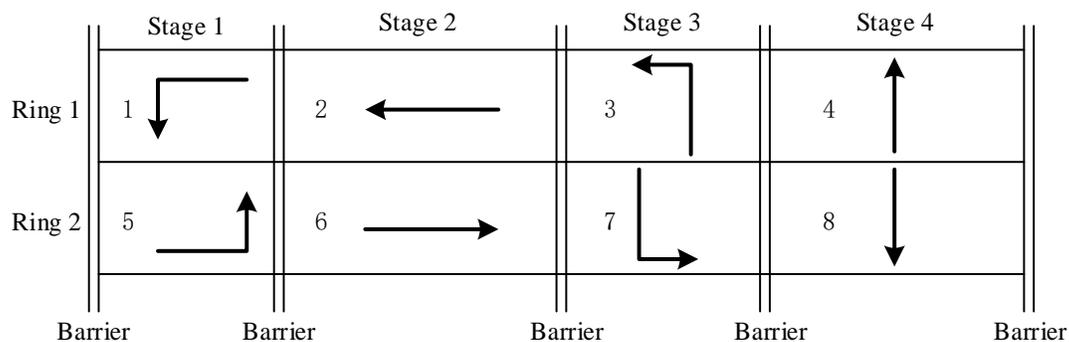

Fig. 1. Ring barrier controller structure with stage definition for a 4-approach intersection.

A barrier is defined as the conflicts between movements. A phase is defined as a controller timing unit associated with the control of one or more movements. A stage, also called phase group is the phases organized by group and separating the crossing or conflicting traffic streams with time between when they are allowed to operate by adding a barrier between the movements. A typical example, as presented in Fig. 1, has 4-stage, 8-phase for a control cycle. Normally, the phases or stages will run continuously step by step following the preset sequence for each cycle.

Due to the sequential nature of signal timing optimization, DP algorithm [11, 26-28] is adopted here to search for an optimal plan based on predicted arrival traffic flow. A DP family algorithm, EOP, is proposed here which aims at minimizing intersection total control delay by considering both minimum/maximum phase green time constraints. In addition, the RO scheme is implemented to roll the timing plan optimization process in a 2-sec time-step by absorbing newly collected traffic data. As a result, even though the signal timing plan is optimized along the fixed prediction time horizon, it is only applied to the field for 2 secs, after that a new timing plan is provided again after the optimization process. The compatibility between subsequent timing plans is ensured.

In this example, the number of stages is four, the number of phases is eight as shown in Fig. 1. TABLE I lists the notation of parameters and variables used in this paper.

TABLE I
NOTATION OF KEY PARAMETERS AND VARIABLES USED TO THIS PAPER.

Variable	Description	Unit
Sets		
B	Set of stages. The cardinality of this set is denoted as $|B|$.	-
P	Set of phases. The cardinality of this set is denoted as $|P|$.	-
S_j	Set of state variables s_j.	-
$X_j(s_j)$	Set of feasible control decisions, given state variable s_j.	-
Parameters		
Input Parameters		
T	Time planning horizon of the sum of all stage, as measured in discrete time intervals of Δ.	seconds
G_i^{min}	Minimum green time for phase i.	seconds
G_i^{max}	Maximum green time for phase i.	seconds
r	Effective clearance interval, the phase change interval which is the total of the yellow change and red clearance times of current phase/stage.	seconds
$A_p(t)$	Number of vehicle arrivals for phase p at time t.	vehicles
SF_p	Saturation flow rate for phase p.	veh·s⁻¹
F	Smoothing factor.	-
Model Variables		
T^E	Expanded time planning horizon, measured in discrete time interval of Δ.	seconds
ξ_i	Green time elapsed for stage i.	seconds
j	Index for stages of the dynamic programming.	-
s_j	State variable denoting the total number of time steps that have been allocated after stage j has completed.	seconds
X_j^{min}	Minimum green time of stage j.	seconds
X_j^{max}	Maximum green time of stage j.	seconds
Ψ_j^1	The possible minimum value of $X_j(s_j)$	seconds
Ψ_j^2	The possible maximum value of $X_j(s_j)$	seconds
$f_j(s_j,x_j)$	Performance measure at stage j, given state variable s_j and control variable x_j.	veh·s
$v_j(s_j)$	Value function (cumulative value of prior performance measures), given state variable s_j.	veh·s

$D_p(t)$	Number of vehicles departing for phase p at time t.	vehicles
$Q_p(t)$	Number of queue vehicles for phase p at time t.	vehicles
$d_p(s_j, x_j)$	Vehicle delay at phase p, given state s_j and control x_j.	veh·s
$g_p(t)$	Signal state for phase p at time t, zero presents clearance signal, one presents green signal.	-
Decision Variables		
x_j	Control variable denoting the amount of green time allocated to stage j, the model's decision variable.	seconds

B. EOP formulation

During the rolling process, there exists a few periods. It can be called as a frozen period when the optimization computation is not needed. These include those periods when a green phase already started but has not reached the minimum green time, and the periods of a clearance interval before reaching the end in the same way. The following section presents the analytical formulas of DP for different stages.

Assuming the current accumulated running stage is i and green time elapsed is ξ_i, the minimum and maximum phase green time for each stage are calculated according to the signal timing parameters as shown in Eqs. (1-2). Let $k = (i + j - 1)\%4$, where symbol % means a mode operation, then we get:

$$X_j^{\min} = \begin{cases} 0 & if\ j = 1 \\ G_4^{\min} & if\ k = 0\ and\ j \geq 2 \\ G_k^{\min} & other \end{cases} \tag{1}$$

$$X_j^{\max} = \begin{cases} G_1^{\max} - \xi_i & if\ j = 1 \\ G_4^{\max} & if\ k = 0\ and\ j \geq 2 \\ G_k^{\max} & other \end{cases} \tag{2}$$

In COP [11], a clearance interval (or called effective red time) is always presented at the end of the time planning horizon T, which is a very restrictive assumption. Therefore, COP does not completely search for the possible timing plans space. But, in EOP, the time planing horizon T is expanded to T^E, which releases the constraints of COP. Considering T^E is not smaller than T, T^E is called expanded time planning horizon. Meanwhile, the arriving vehicle is set to 0 for time period beyond time horizon T as shown in Fig.2.
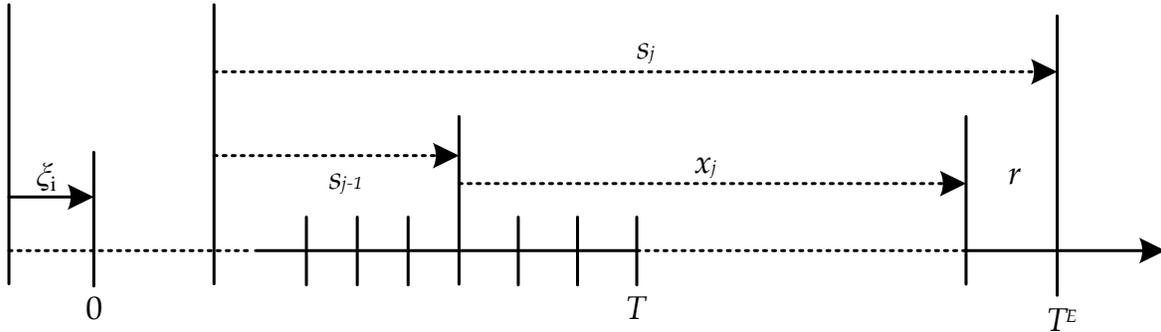
**Fig. 2.** Relationship between the elapsed green time (ξ_i), state variables (s_{j-1}, s_j), decision variable (x_j), clearance interval (r), total number of discrete time-steps (T), and expanded total number of discrete time-steps (T^E).

Proper selection of T^E could not only cover all possible solutions, but also reduce computation time. The selection method is explained as follows. COP does not allow green time to be left at the end of T when it is less than the minimum green time of the following stage. It simply adds that time to the previous phase. Referring to the least common multiple idea, a method as presented in Eqs. (3-4) is developed to expand the prediction time horizon long enough to include a completely new phase. Therefore, there will be enough time to provide both green and clearance intervals which will satisfy the condition of applying COP.

$$\sum_{j=2}^{\zeta_1^*-1}\left(X_j^{\min}+r\right) \leq T-r < \sum_{j=2}^{\zeta_1^*}\left(X_j^{\min}+r\right) \tag{3}$$

$$\sum_{j=1}^{\zeta_2^*-1}\left(X_j^{\max}+r\right) \leq T < \sum_{j=1}^{\zeta_2^*}\left(X_j^{\max}+r\right) \tag{4}$$

The expanded time planning horizon T^E is determined by searching for values of ζ_1^* and ζ_2^* that both meet the constraints described by Eqs. (3) and (4), and the following criteria of Eq. (5).

$$T^E = \max\left(\sum_{j=2}^{\zeta_1^*}\left(X_j^{\min}+r\right)+r, \sum_{j=1}^{\zeta_2^*}\left(X_j^{\max}+r\right)\right) \tag{5}$$

A simple example is presented here to illustrate the DP process. Assuming signal control includes three stages: A, B, C, and some parameters as, $T = 10$ secs, $G^{\min} = 2\ secs$, $G^{\max} = 4\ secs$, $r = 1\ sec$, $i = 1$. Then, a method of decision tree is used here to explain the DP process as shown in Fig.3. First, based on Eqs. (1-5), the expanded optimization time horizon is calculated, $T^E = 13$ secs. Following that, the DP process is described as a decision tree shown in Fig.3.
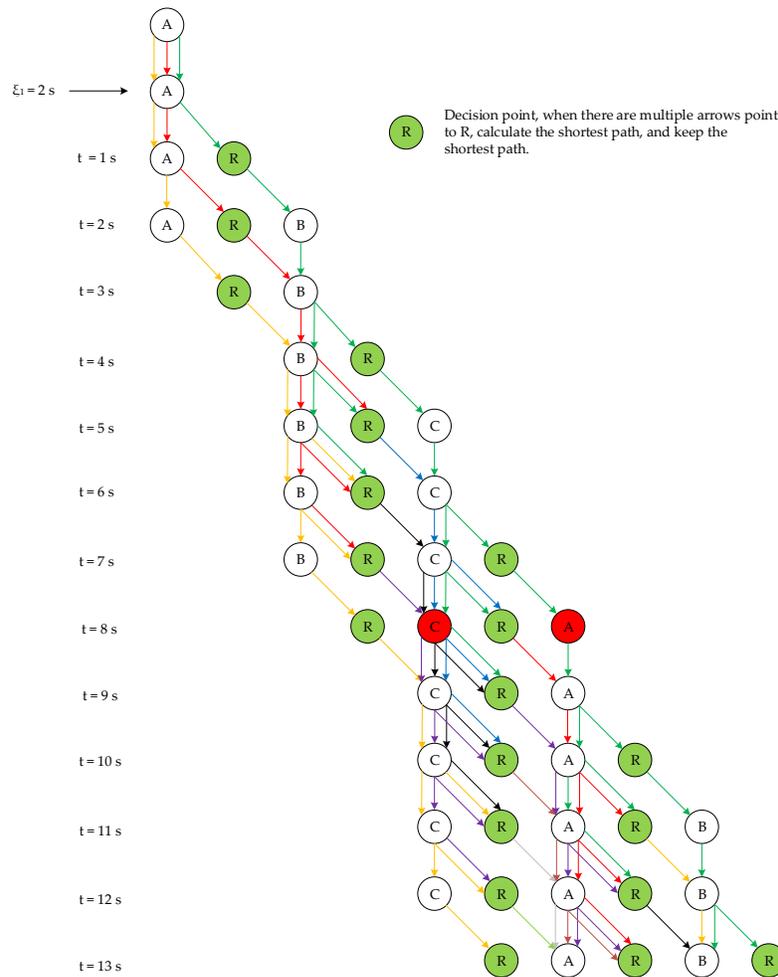
Fig. 3. An example of a signal timing plan decision tree.

In Fig. 3, different colored arrows represent different paths. The point marked in green color R is a decision point. The utility value of these paths is computed when there are multi-paths arrive this decision point. Then, the minimum utility value of the path is saved together with its path sequence, other paths are ignored. Therefore, only one arrow departs from the decision point. For example, when $t = 6s$, there are three paths arrive the green decision point R. The green arrow path is A→A→R→B→B→B→B→R, the yellow arrow path is A→A→A→A→R→B→B→R, and the red arrow path is A→A→A→R→B→B →B→R. Then, the utility value of these three paths are computed and the minimum one path is retained and through the green decision point. Other two paths are stoped at the green decision point.

Since there are only 10 secs data in this example, the COP only considers the integer stage solutions which imply these plans must stop at the decision point (clearance time point R). Therefore, the process will be truncated at time 10 secs when applying the COP, which is marked as the red color, and all enumerated possible timing plans are listed in TABLE II. There are only 4 integer stage plans checked, because other plans not ended with clearance time (i.e., not integer stage plans) are not considered. However, by following the EOP algorithm, the prediction time horizon is firstly expanded, then, all possible timing plans without the constraint of ending with clearance time are fully enumerated as listed in TABLE III.

TABLE II
EMULATED SIGNAL TIMING PLANS IN COP (SEC).

Plan ID	Signal Timing Plan	Plan ID	Signal Timing Plan
1	[2 + 1,2 + 1,3 + 1]	3	[3 + 1,2 + 1,2 + 1]
2	[2 + 1,3 + 1,2 + 1]	4	[4 + 1,4 + 1]

TABLE III

EMULATED SIGNAL TIMING PLAN IN EOP (SEC).

Plan ID	Signal Timing Plan	Equivalent signal timing plan in 10 s period
1	[2 + 1,2 + 1,2 + 1,2 + 1,2 + 1]	[2 + 1,2 + 1,2 + 1,1 + 0]
2	[2 + 1,3 + 1,3 + 1,3 + 1]	[2 + 1,3 + 1,3 + 0]
3	[3 + 1,2 + 1,3 + 1,3 + 1]	[3 + 1,2 + 1,3 + 0]
4	[3 + 1,3 + 1,2 + 1,3 + 1]	[3 + 1,3 + 1,2 + 0]
5	[3 + 1,3 + 1,3 + 1,2 + 1]	[3 + 1,3 + 1,2 + 0]
6	[2 + 1,2 + 1,3 + 1,4 + 1]	[2 + 1,2 + 1,3 + 1]
7	[2 + 1,2 + 1,4 + 1,3 + 1]	[2 + 1,2 + 1,4 + 0]
8	[4 + 1,2 + 1,2 + 1,3 + 1]	[4 + 1,2 + 1,2 + 0]
9	[3 + 1,2 + 1,2 + 1,4 + 1]	[3 + 1,2 + 1,2 + 1]
10	[3 + 1,4 + 1,2 + 1,2 + 1]	[3 + 1,4 + 1,1 + 0]
11	[4 + 1,3 + 1,2 + 1,2 + 1]	[4 + 1,3 + 1,1 + 0]
12	[2 + 1,4 + 1,2 + 1,3 + 1]	[2 + 1,4 + 1,2 + 0]
13	[2 + 1,3 + 1,2 + 1,4 + 1]	[2 + 1,3 + 1,2 + 1]
14	[4 + 1,2 + 1,3 + 1,2 + 1]	[4 + 1,2 + 1,2 + 0]
15	[3 + 1,2 + 1,4 + 1,2 + 1]	[3 + 1,2 + 1,3 + 0]
16	[2 + 1,3 + 1,4 + 1,2 + 1]	[2 + 1,3 + 1,3 + 0]
17	[2 + 1,4 + 1,3 + 1,2 + 1]	[2 + 1,4 + 1,2 + 0]
18	[4 + 1,4 + 1,4 + 1]	[4 + 1,4 + 1]

This example shows that the COP algorithm may not be capable of finding the optimal solution due to non-exhaustive searching in the solution space.

Then, given the state j and the calculated minimum and maximum green time allowed for that stage and the total discrete time-steps, the set of state variables is determined by Eq. (6).

$$S_j = \begin{cases} r, \cdots, \min(X_i^{\max} + r, T^E) & if \ j = 1 \\ \sum_{m=i+1}^{i+j-1}(X_m^{\min} + r) + r, \cdots, \min\left(\sum_{m=i}^{i+j-1}(X_m^{\max} + r), T^E\right) & if \ j \geq 2 \end{cases} \tag{6}$$

where, $\sum_{m=i+1}^{i+j-1}(X_m^{\min} + r) + r$ is the minimum time length before stage j, and $\sum_{m=i}^{i+j-1}(X_m^{\max} + r)$ is the maximum time length before stage j. When phase jump is not considered, the state variable S_j is only related to the state, but not necessarily in the range between 1 and T^E, which is discrete values as in Eq. (6). The same for the expanded optimization time horizon of T^E, the value of S_j can't exceed T^E. Therefore, the state variable S_j is the minimum of the two maximum values, $\min\left(\sum_{m=i}^{i+j-1}(X_m^{\max} + r), T^E\right)$.

Given the state variable s_j and the calculated minimum and maximum green time allowed for the stage, the set of feasible control variables is determined by Eqs. (7-9).

$$X_j(s_j) = \begin{cases} 0, \cdots, X_j^{\max} & if \ j = 1 \\ \Psi_j^1, \cdots, \Psi_j^2 & if \ j \geq 2 \end{cases} \tag{7}$$

$$\Psi_j^1 = \max\left\{X_j^{\min}, s_j - \sum_{m=1}^{j-1}(X_m^{\max} + r) - r\right\} \qquad (8)$$

$$\Psi_j^2 = \min\left\{X_j^{\max}, s_j - \sum_{m=2}^{j-1}(X_m^{\min} + r) - 2r\right\} \qquad (9)$$

After determining the formulas of S_j and $X_j(s_j)$, DP is used to search for the best timing plan. The process includes two stages, the first stage is called Forward recursion, which calculates the optimal value of the target function in every time step; the second stage is called Backward recursion, which finds the timing plan corresponding to the optimal value of the target function.

C. EOP Search Process

The forward and backward recursion of the EOP is described.

I. Forward recursion

Step 1: Set $j = 1$, $s_{j-1} = 0$ and $v_j(0) = 0$.
Step 2: Calculate S_j.
Step 3: For s_j in S_j {
　　　　Calculate $X_j(s_j)$.
$$v_j(s_j) = \text{Min}_{x_j}\{f_j(s_j, x_j) + v_{j-1}(s_{j-1})|x_j \in X_j(s_j)\}$$
　　record $x_j^*(s_j)$ as the optimal solution in Step 2.
　　}.
Step 4: If $(\sum_{k=2}^{(j+1)}(X_k^{\min} + r) + r \le T^E)$, $j = j + 1$, go to Step 2.
Else STOP.

The forward recursion starts with assigning the first stage as 1 and the cumulative value function as 0 at the beginning of the optimization time horizon. For each stage, the EOP calculates the optimal decision $x_j^*(s_j)$ for each state variable s_j. The objective function $f_j(s_j, x_j)$ is used to determine the state variable is passed to the lower optimization level with the constraint of control variable x_j. The calculated progress will be discussed in section D. The stopping criteria is met if the minimum s_j is greater than T^E. The cumulative value function cannot be improved within the period of four phase groups. The justification of the stopping criterion is different from that in [11], which does not consider constraint of the maximum green time of a phase group.

II. Backward recursion

After all decisions are made for all stages, the optimal decision $x_j^*(s_j)$ of each stage can be retrieved in the backward recursion as follows.

First, search for the minimum delay $v_{j^*}^*(T^*)$ corresponding to state variable $s_j^* = T : T^E$, and record $J = j^*$.

Step 1: Find the minimum $v_j(t)$, $t \in [T, T^E]$, record $v_{j^*}^*(T^*)$.
Step 2: Set $J = j^*$ and $s_j^* = T^*$.
Step 3: For $j = J, J - 1, \cdots, 1$ {
　　　Read $x_j^*(s_j^*)$ from the table computed in forward recursion.
　　　　If $(j > 1)$, $s_{j-1}^* = s_j^* - x_j^*(s_j^*) - r$.
}.

The optimal plan is retrieved from stage $J = j^*$ since this stage denotes the minimum $v_{j^*}^*(T^*)$, such as the minimum delay or stops. In COP algorithm, the optimal plan must meet the integer stages, so the last stage stops at time T, but in the EOP algorithm, the last stage of the optimal plan stops at the range of time internal $[T, T^E]$. So, compared to the COP algorithm, the proposed EOP algorithm can obtain the optimal signal timing plan given the prediction vehicle arrivals [15].

D. Calculation of performance indices

A signal phase except the red interval is assumed to have two signal indications: green signal and clearance signal (yellow and all red signal). Once the timing plan is given, then, the signal indication of phase p at time t is represented by $g_p(t)$ [28], which is denoted as follows.

$$g_p(t) = \begin{cases} 0, & \text{clearance signal or red signal} \\ 1, & \text{green signal} \end{cases}, t \in [1, T], p \in P. \tag{10}$$

Based on the IQA method [30], as for phase p, the number of queuing vehicles $Q_p(t)$ of the current time t is related to the number of queueing vehicles $Q_p(t-1)$ of the last time $t-1$, the number of arrived vehicles $A_p(t)$ and the number of departed vehicles $D_p(t)$ of the current time t.

$$Q_p(t) = Q_p(t-1) + A_p(t) - D_p(t), t \in [1, T], p \in P, \tag{11}$$

where, $D_p(t)$ is the number of departed vehicles at time t of phase p, and $Q_p(0) = 0$.

As for phase p in Eq. (11), the number of arrived vehicles $A_p(t)$ and the number of queuing vehicles $Q_p(t-1)$ are known. While $D_p(t)$ is related to the signal indication of phase p and the saturated leaving flow rate. The following section presents the computation process of $D_p(t)$ in three situations.

Therefore, the formula to calculate $D_p(t)$ is as follows.

$$D_p(t) = \begin{cases} 0 & \text{if } g_p(t) = 0 \\ A_p(t) + Q_p(t-1) & \text{if } g_p(t) = 1 \text{ and } A_p(t) + Q_p(t-1) \le SF_p \\ SF_p & \text{if } g_p(t) = 1 \text{ and } A_p(t) + Q_p(t-1) > SF_p \end{cases}, t \in [1, T], p \in P. \tag{12}$$

Given s_j and x_j, $D_p(t)$ can be obtained using Eq. (7) for $t \in [s_{j-1} + 1, s_j]$, and $Q_p(t)$ can be obtained using Eq. (11). Using the IQA method, the total delay $d_p(s_j, x_j)$ of phase p can be computed as follows.

$$d_p(s_j, x_j) = \sum_{t=s_{j-1}+1}^{\min(s_j, T)} Q_p(t) \tag{13}$$

Given s_j, x_j, the total delay of time-interval $[s_{j-1}, s_j]$ is calculated by adding up those delay associated with each phase p, that is,

$$f_j(s_j, x_j) = \sum_{p \in P} d_p(s_j, x_j) \tag{14}$$

Therefore, the following can be derived based on Eqs. (13-14).

$$f_j(s_j, x_j) = \sum_{p \in P} \sum_{t=s_{j-1}+1}^{\min(s_j, T)} Q_p(t) \tag{15}$$

The optimization model for each stage can be summarized as follows.

$$\min \sum_{p \in P} d_p(s_j, x_j) \tag{16}$$

s.t.

$$d_p(s_j, x_j) = \sum_{t=s_{j-1}+1}^{\min(s_j, T)} Q_p(t), p \in P. \tag{17a}$$

$$D_p(t) = \begin{cases} 0 & if\ g_p(t) = 0 \\ A_p(t) + Q_p(t-1) & if\ g_p(t) = 1\ and\ A_p(t) + Q_p(t-1) \le SF_p, t \\ SF_p & if\ g_p(t) = 1\ and\ A_p(t) + Q_p(t-1) > SF_p \end{cases} \tag{17b}$$
$$\in [s_{j-1} + 1, \min(s_j, T)].$$

$$Q_p(t) = Q_p(t-1) + A_p(t) - D_p(t), t \in [s_{j-1} + 1, \min(s_j, T)], p \in P. \tag{17c}$$

$$\begin{cases} G_p^{\min} \le \displaystyle\sum_{t=s_{j-1}+1}^{s_j} g_p(t) \le G_p^{\max} & if\ s_j \le T \\ 1 \le \displaystyle\sum_{t=s_{j-1}+1}^{T} g_p(t) \le G_p^{\max} & if\ s_j > T \end{cases} \quad p \in P. \tag{17d}$$

where, Eq. (17d) includes the constraints of minimum and maximum green time. If the time of the end of the last stage is within the optimization time horizon, the green time needs to satisfy the minimum and maximum green time constraints. Else if the time of the end of the last stage exceeds the optimization time horizon, then, the phase green time no needs to satisfy the minimum green time constraint, but just needs to satisfy the sum of running green time and the green time at the beginning of the next optimization is greater than the minimum green time of the phase.

E. An RO solution based on cross-sectional VII data

If the vehicle arriving distributions of all phases are known, an RO scheme can be applied for signal timing optimization. The flowchart of the RO process is presented in Fig.4. The flowchart includes a key part: EOP algorithm. To illustrate the EOP algorithm, a simple illustrative example is presented in section IV. In addition, the more details of vehicle arriving distributions for EOP algorithm in a cross-sectional VII environment can refer to [15].
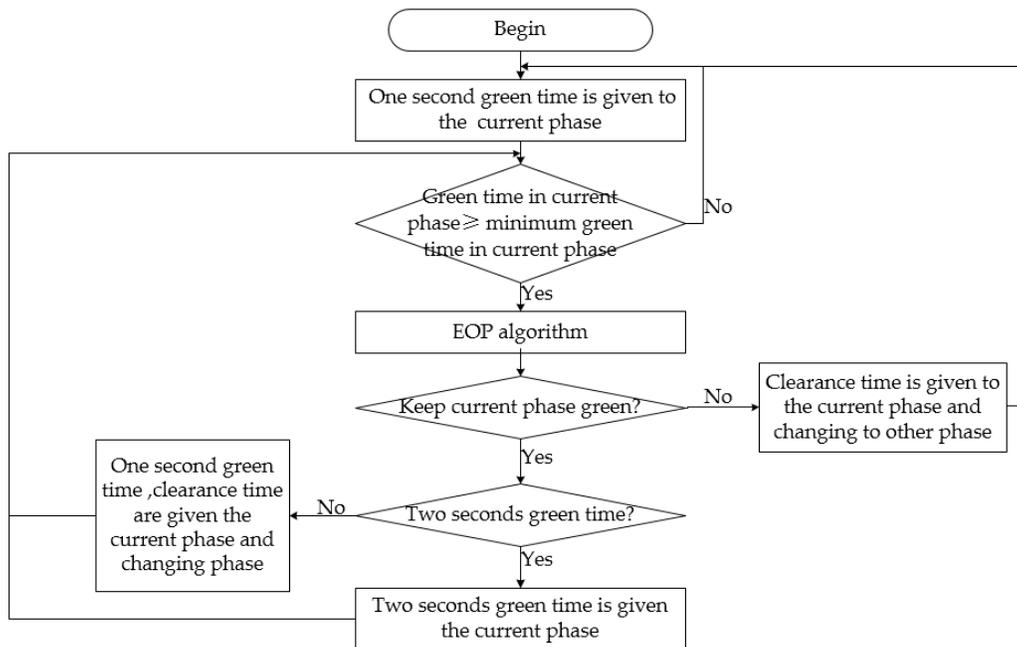
Fig. 4. Flow chart of the RO process.

As shown in Fig.4, the RO process includes the following three steps.

Step 1. Check the current phase for whether it has reached the minimum green time or not. If not, then extend the green interval for one more time step; if yes, then go to **Step 2**.

Step 2. According to the EOP algorithm, there are only three scenarios after the optimization, that is, extend green interval for 2 secs, 1 sec, or terminate the green interval.

Step 3. If extend the green interval for 2 secs, then go to step 2; if extend for 1 s, then start the clearance interval, change the signal phase, and go to **Step 1**; if terminate the green interval, then start the clearance interval, and go to **Step 1**.

IV. AN ILLUSTRATIVE EXAMPLE

A typical intersection is used to illustrate the proposed optimization process, which has 8 phase and 4 phase groups (**Fig. 1**). The operating sequence of the phase groups is $A, B, C, D, A, B, C, D, \cdots$ with starting phase group of A. We assume the optimization time period $T = 10$ secs. The vehicle arrives of the future of 10 secs are shown in TABLE V. Also, we assume the same minimum green time $G^{\min} = 2\ secs$, the maximum green time $G^{\max} = 4\ secs$, clearance interval period $r = 1\ secs$, the saturated flow rate $SF = 2veh \cdot s^{-1}$ for all phases.

Clearly, at the beginning, it does not satisfy the rolling optimization condition. Until $t = 2$, then $\xi^1 = 2 \geq X_1^{\min}$ which meets the rolling optimization condition. The initial queue of each phase is computed based on the vehicle arriving data of the first 2 secs as shown in TABLE IV.

TABLE IV

INITIAL QUEUE FOR ALL PHASES.

P1	P2	P3	P4	P5	P6	P7	P8
0	1.87	0.56	1.30	0	0.26	0.14	0.32

Then, following Eqs. (3-5), the expanded optimization time horizon is determined as $T^E = 13\ secs$, after setting the vehicle arrivals as 0 for time period beyond 10 secs, the final arriving vehicle distribution table is as shown in TABLE V.

TABLE V
EXPAND ARRIVAL DATA FOR ALL PHASES IN THE OPTIMIZATION RANGE.

Time	P1	P2	P3	P4	P5	P6	P7	P8
1	0.18	0.43	0.34	0.80	0.08	0.18	0.22	0.52
2	0.41	0.96	0.17	0.41	0.24	0.56	0.30	0.70
3	0.06	0.13	0.33	0.78	0.17	0.39	0.11	0.26
4	0.32	0.75	0.20	0.47	0.44	1.02	0.22	0.50
5	0.10	0.23	0.28	0.65	0.26	0.61	0.04	0.10
6	0.33	0.76	0.34	0.79	0.04	0.10	0.03	0.08
7	0.01	0.01	0.27	0.64	0.03	0.06	0.40	0.93
8	0.31	0.71	0.04	0.08	0.17	0.39	0.19	0.44
9	0.04	0.09	0.20	0.46	0.13	0.29	0.09	0.21
10	0.26	0.62	0.11	0.25	0.41	0.96	0.30	0.70
11	0	0	0	0	0	0	0	0
12	0	0	0	0	0	0	0	0
13	0	0	0	0	0	0	0	0

By following Equation (6), we can compute: $S_1 = \{1,2,3\}$, and $X_1(1) = \{0\}, x_1^*(1) = 0$; $X_1(2) = \{1\}, x_1^*(2) = 1$; $X_1(3) = \{2\}, x_1^*(3) = 2$, results are as shown in TABLE VI.

TABLE VI
CALCULATION FOR STAGE 1.

s_1	$x_1^*(s_1)$	$v_1(s_1)$	$Q_{s_1}^1$	$Q_{s_1}^2$	$Q_{s_1}^3$	$Q_{s_1}^4$	$Q_{s_1}^5$	$Q_{s_1}^6$	$Q_{s_1}^7$	$Q_{s_1}^8$
1	0	7.18	0.18	2.29	0.90	2.09	0.08	0.44	0.36	0.84
2	1	17.59	0.41	3.26	1.07	2.50	0.24	1.00	0.66	1.55
3	2	29.19	0.06	3.39	1.41	3.28	0.17	1.39	0.77	1.80

Then, by following Eq. (6), for stage 2, we can compute: $S_2 = \{4,5,6,7,8\}$. As an example, for $s_2 = 7$, we can compute: $X_2(7) = \{3,4\}$. When $x_2 = 3$, we can get: $s_1 = s_2 - x_2 - r = 3$. Meanwhile, by following Eqs. (8-11), we can get: $f_2(7,3) = 51.26$. By analogy, the sample process can be applied for $x_2 = 4$. The results are listed in TABLE VII, which shows the minimum value of $v_2(s_2)$ is $f_2(s_2,x_2) + v_1(s_1) = 78.18$, then, $x_2^* = 4$. The sample process applies for $s_2 = 4,5,6,8$, as presented in TABLE VIII.

TABLE VII
VALUE FUNCTION FOR STAGE 2.

x_2	$f_2(7,x_2)$	s_1	$v_1(s_1)$	$f_2 + v_1$
3	51.26	3	29.19	80.45
4	60.59	2	17.59	78.18

TABLE VIII
CALCULATION FOR STAGE 2.

s_2	$x_2^*(s_2)$	$v_2(s_2)$	$Q_{s_2}^1$	$Q_{s_2}^2$	$Q_{s_2}^3$	$Q_{s_2}^4$	$Q_{s_2}^5$	$Q_{s_2}^6$	$Q_{s_2}^7$	$Q_{s_2}^8$
4	2	35.79	0.97	0.75	1.59	3.75	0.93	1.02	0.99	2.30
5	2	50.19	0.89	0.37	1.87	4.40	1.11	0.61	1.03	2.40
6	4	62.25	1.40	5.13	2.21	0.79	1.23	3.12	1.06	0.08

| 7 | 3 | 80.45 | 0.82 | 0.01 | 2.48 | 5.83 | 0.94 | 0.06 | 1.46 | 3.41 |
| 8 | 4 | 97.65 | 1.13 | 0.71 | 2.52 | 5.91 | 1.11 | 0.39 | 1.65 | 3.85 |

Following the previous process, we can compute the target value of each stage, then, according to the stop criteria, as for the time $j = 5$, the optimization process reaches the end. The target value of each stage is listed in TABLE IX and the value of all variables in TABLE X.

TABLE IX
VALUE FUNCTION FOR ALL STAGES.

s	v_1	v_2	v_3	v_4	v_5
1	7.18	—	—	—	—
2	17.59	—	—	—	—
3	29.19	—	—	—	—
4	—	35.79	—	—	—
5	—	50.19	—	—	—
6	—	61.25	—	—	—
7	—	80.45	77.35	—	—
8	—	97.65	79.55	—	—
9	—	—	93.08	—	—
10	—	—	126.53	119.33	—
11	—	—	116.34	107.81	—
12	—	—	116.34	103.83	—
13	—	—	130.21	100.54	154.09

As shown in TABLE V, the minimum value of those rows 10-13 is $v_4(13)$, $s_4^* = 13$, and $x_4^*(s_4^*) = 4$. Since $s_3^* = s_4^* - x_4^*(s_4^*) - r = 8$, then, $x_3^*(8) = 3$. Accordingly, we can get: $x_2^*(4) = 2$, $x_1^*(1) = 0$. The timing plan of the first 10 s (3-12s) is: phase group A: green 0 sec[2], clearance 1 sec; phase group B: green 2 secs, clearance 1 sec; phase group C: green 3 secs, clearance 1 sec; phase group D: green 2 secs, clearance 0 sec. Due to the rolling optimization scheme, the optimized plan will be implemented as follows: phase group A operates for 1 sec clearance interval, then, phase group B operates for a period of its minimum green interval. When the phase group B has run for its minimum green interval, the rolling optimization process is implemented again by integrating newly collected traffic data. If optimization results are extending the green interval for 2 secs, then, the minimum and maximum green intervals constrain will be adjusted/reduced since that phase has already run for some green time.

TABLE X
DECISION TABLE FOR ALL STAGES.

s	$j = 1$	$j = 2$	$j = 3$	$j = 4$	$j = 5$
1	0	—	—	—	—
2	1	—	—	—	—
3	2	—	—	—	—
4	—	2	—	—	—
5	—	2	—	—	—
6	—	4	—	—	—
7	—	3	2	—	—
8	—	4	3	—	—
9	—	—	3	—	—
10	—	—	2	2	—

[2] This situation means the phase group A does not require green time, the intersection run all-red phase to clear the intersection.

11	—	—	3	2	—
12	—	—	4	3	—
13	—	—	4	4	2

V. CASE STUDY AND DISCUSSION

The cross-sectional VII environment is modeled in traffic micro-simulation software, VISSIM [31], DPDM [15] is used to predict the arriving vehicles based on speed data of the upstream VII cross-sectional, and the proposed optimization method is built through COM technology. The optimized signal timing parameters are then applied to signal controller in real-time, also model performance data is collected for model evaluation. The framework of the simulation experiment is presented in Fig. 6.

In a real road network, vehicles are equipped with OBUs that is able to communicate with the RSUs in a cross-sectional VII environment. In a VISSIM simulation environment, the loop detectors are used to model the cross-sectional VII environment which gathers the speed data at the upstream cross-section. The control system has two components: dynamic platoon dispersion model and EOP algorithm. The dynamic platoon dispersion model (DPDM) proposed platoon dispersion model based on real-time cross-section VII data, which predicts vehicle arrivals in real time, with more details in [15]. Then, the output of the EOP algorithm is the optimal signal duration for each phase. The optimal solution is then converted to a list of signal control events and sent to the signal control interface.

A real road network is modeled in VISSIM, which includes 5 signalized intersections. In order to model the cross-sectional VII environment, detectors in VISSIM is set up at the predefined upstream cross-section to collect vehicles' speed and time stamp information when they pass the location. Later, that information is forwarded to the optimization program through COM connection [32]. Based on the real-time speed data, DPDM [15] predicts the arriving flow distribution at downstream stop-line. Then, the signal controller adjusts the signal timing parameters according to the optimization results in real time.
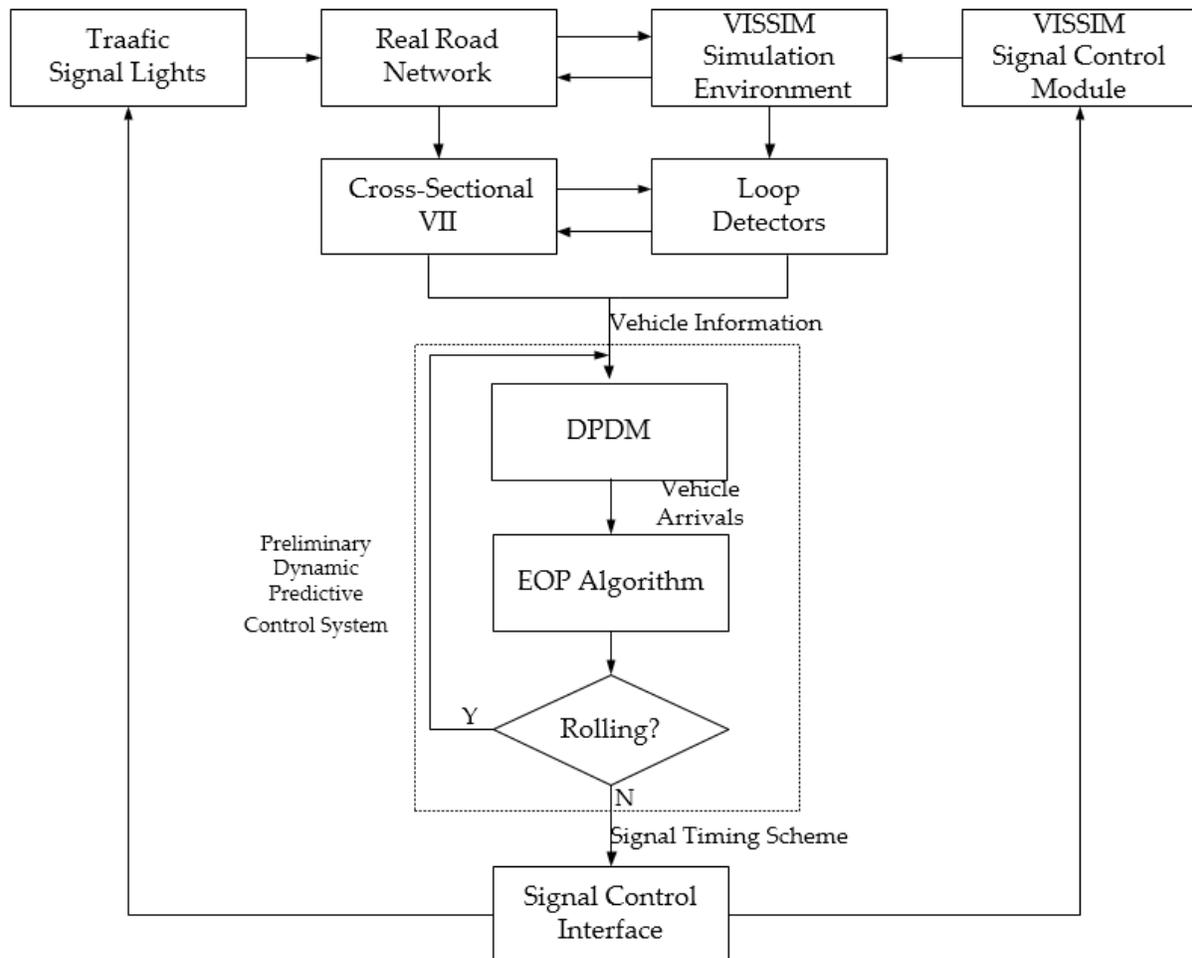
Fig. 6. Framework for a simulation experiment.

For comparison, full-actuated control after parameters optimization is used as the background to evaluate the performance of the dynamic prediction control system. Intersection delay, which can be easily obtained in VISSIM, is chosen as the main evaluation criteria.

A. Case study

Fig. 7 presents a real road network at the City of Chengdu, China, which has a typical grid structure. Geometric data is collected in the field in order to reflect the field condition, and is further coded into VISSIM. There are totally 5 intersections; the one numbered 5 is chosen as the testing intersection for the proposed control system as shown in Fig. 7. Full actuated control is applied to all the other intersection. Cross-sectional VII is set up at all 4 upstream locations for the testing intersection. As a reasonable simplification, no right-turn traffic is modeled in this study, only through and left-turn traffic flow is modeled [11, 25]. So, the turning percentages of the case intersection are listed in TABLE XI.

TABLE XI
THE TURNING PERCENTAGES (%) OF THE STUDY INTERSECTION.

Node	1	2	3	4
1	-	32	68	-
2	-	-	26	74
3	63	-	-	37
4	38	62	-	-

Simulation pre-warm time is set at 900 secs, and effective simulation time is 3600 secs. Different traffic volume levels are modeled in VISSIM in order to test the compliance of the proposed control system to real traffic conditions. The average delay and the average queue length of two control methods are collected from simulation data and plotted in Fig.8 to compare the performance of the two methods.
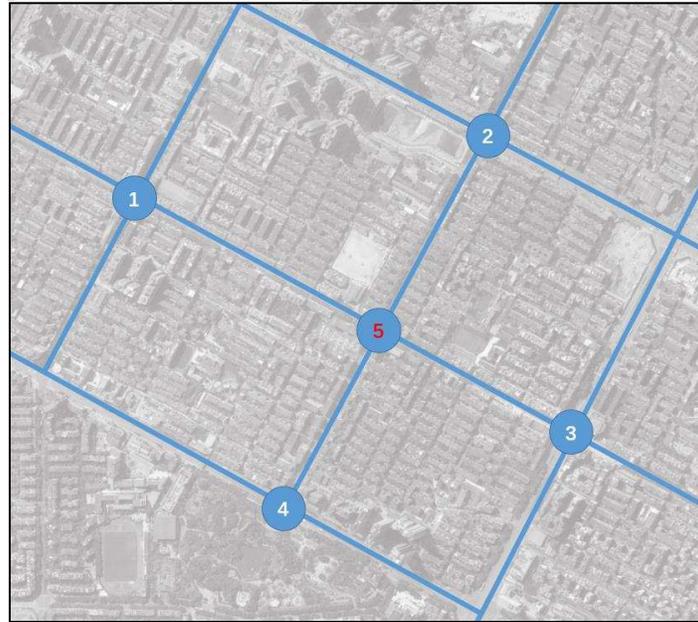

a) Road network

b) The controlled intersection

Fig. 7. Road network of the case study.
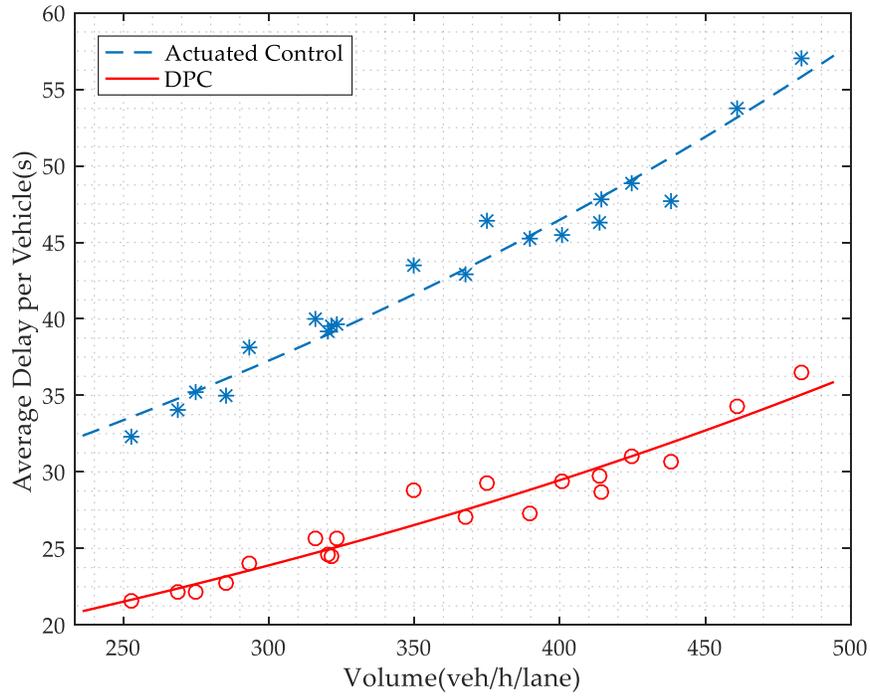
(a) Average vehicle delay
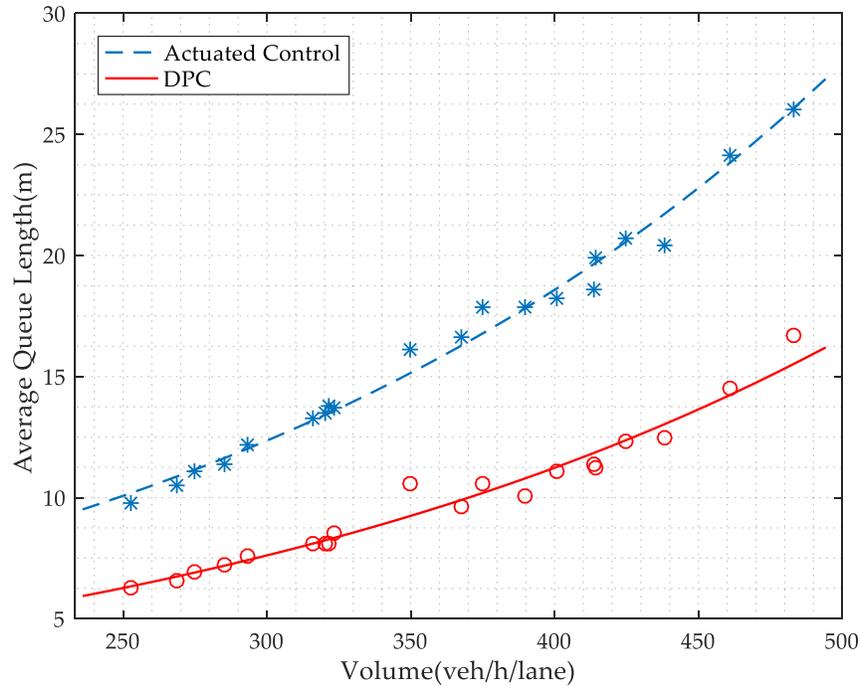
(b) Average queue length

Fig. 8. Delay and queue length versus volume for full-actuated control and the proposed control system.

As shown in Fig. 8(a), the average vehicle delay increases as traffic volume increases. Comparing to full-actuated control, the proposed control system always has lower average vehicle delay. The similar result is observed when comparing the average queue length, as shown in Fig. 8 (b). It can be concluded that the proposed control system demonstrates improvement comparing to traditional full-actuated control.

B. Discussion of result

Detailed performance data of the two control methods for each phase under four volume levels (250 veh/h/lane, 333 veh/h/lane, 417 veh/h/lane, and 500 veh/h/lane) is listed in TABLE XII and TABLE XIII.

As shown in TABLE XII and TABLE XIII, reduction of average delay and average queue length are observed for all phases. For the studied intersection, the proposed control system can reduce up to 33% of the average vehicle delay and 35% of the average queue length compared to the full-actuated control, proving the effectiveness of the proposed control system.

Meanwhile, the variance of the average delay and queue length is calculated and listed in TABLE XIV. It can be seen from TABLE XIV that the variance of the proposed control system is lower than that of the full-actuated control when traffic volume is low and higher when the traffic volume is high. It means the proposed control system will sacrifice some balance among movements in order to achieve the overall optimal performance. Therefore, multiple objectives including stops, queue length, and balance among movements will help improve the optimization performance which should be considered in future work.

TABLE XII

COMPARISON OF AVERAGE VEHICLE DELAY (SEC/VEH) IN EACH PHASE UNDER DIFFERENT VOLUME LEVELS (VEH/H/LANE).

Volume	Phase 1	Phase 2	Phase 3	Phase 4	Phase 5	Phase 6	Phase 7	Phase 8	Average	Improvement
250	41.4/24.0	27.4/18.1	39.5/27.9	28.7/19.6	38.2/24.9	28.2/19.3	40.8/29.3	29.5/19.1	34.21/22.78	-33.43%
334	54.1/32.6	35.1/26.7	51.1/37.0	37.6/23.2	40.6/25.1	32.8/18.5	43.6/27.7	33.4/19.6	41.04/26.30	-35.91%
417	59.4/36.5	42.2/25.4	58.1/40.9	46.9/26.1	50.6/30.8	42.4/23.4	58.3/35.1	40.4/24.2	49.79/30.30	-39.14%
500	63.5/38.6	51.1/29.4	67.7/56.4	50.4/28.9	59.1/36.8	56.2/30.6	66.5/64.2	54.2/27.9	58.59/39.10	-33.26%

Note: The values are: Average vehicle delay under actuated control / dynamic predictive control.

TABLE XIII

COMPARISON OF AVERAGE QUEUE LENGTH (M) IN EACH PHASE UNDER DIFFERENT VOLUME LEVELS (VEH/H/LANE).

Volume	Phase 1	Phase 2	Phase 3	Phase 4	Phase 5	Phase 6	Phase 7	Phase 8	Average	Improvement
250	8.9/5.1	9.8/6.2	11.4/7.7	9.4/6.5	8.1/5.1	10.5/6.6	9.8/6.8	10/6.4	9.74/6.30	-35.30%
334	16.3/9.0	15.1/11.1	20.7/13.7	16.2/9.7	8.2/5.1	11.8/6.6	10.1/6.2	11/6.8	13.68/8.53	-37.66%
417	20.9/11.4	19.9/11.8	25.5/16.5	21.1/11.1	14.1/8.1	19.9/10.2	20.8/11.1	17.3/9.5	19.94/11.21	-43.76%
500	23/12.3	25.7/14	30.1/26.4	24.6/12.8	19.9/11.8	30.5/15	28.4/29.1	26.1/12.2	26.04/16.70	-35.86%

Note: The values are: Average queue length under actuated control / dynamic predictive control.

TABLE XIV

VARIANCE OF AVERAGE VEHICLE DELAY AND QUEUE LENGTH (M) FOR EACH PHASE UNDER DIFFERENT VOLUME LEVELS (VEH/H/LANE).

Volume	250	334	417	500
Actuated control	39.15/0.99	64.56/16.87	63.32/10.71	45.44/13.01
Dynamic predictive control	18.91/0.75	39.01/8.40	42.94/6.00	190.09/48.12

Note: The values are: Variance of average vehicle delay for each phase/ Variance of average queue length for each phase.

VI. CONCLUSIONS AND FUTURE WORK

A. Conclusion

In this paper, a dynamic predictive control framework is proposed for traffic signal control in a cross-sectional VII environment, which applies EOP algorithm to update timing plan in real time based on short-term predicted traffic flow. In the cross-sectional VII, the distribution of arrival traffic at downstream stop-line is predicted using DPDM. The EOP algorithm uses a full enumeration method to search for the optimal timing plan under the minimum and maximum green time constraints with the objective of

minimizing delay. Meanwhile, the RO scheme is adopted to dynamically optimize the timing plan by integrating newly collected data, which can be applied in a rolling horizon of 2 secs.

Simulation study of a real road network is carried out in VISSIM to test the performance of the proposed method. COM technique is used to communicate with VISSIM from outside the program. Full-actuated control is selected to be compared with the proposed control method. Results show that the proposed method can reduce up to 33% of the average delay and 35% of the average queue length. Traffic detection environment and the dynamic platoon dispersion models make it possible for signal control system to have short-term prediction capability which contributes to a new generation of signal control which is the dynamic predictive signal control framework.

B. Future work

Predictive signal control for single intersection actually applies the implicit coordination between subsequent intersections; future work can explore the explicit coordination control (with coordinated green bands) in a VII environment. Besides, there are still some open areas worth investigation, such as: combined objectives (including stops, queue lengths et al.) optimization to achieve more balanced signal control plans; multi-cross-sectional VII environment to improve the accuracy of traffic flow prediction; and feedback strategy to gain more robust control by using the post-event vehicle's control delay, queueing and turning movements data et al. supported by VII technology.

REFERENCES

[1] F. V. Webster and B. M. Cobbe, "Traffic signals," Her Majesty's Stationery Office, London, U.K., Road Research Tech. Rep. 39, 1958.

[2] M.J. Smith, R. Liu, and R. Mounce, "Traffic control and route choice: Capacity maximisation and stability," *Transp. Res. B, Methodol*, vol. 81, no. 3, pp. 863-885, Nov. 2015.

[3] R. Liu, and M. Smith. "Route choice and traffic signal control: a study of the stability and instability of a new dynamical model of route choice and traffic signal control," *Transp. Res. B, Methodol,* vol. 77, pp. 123-145, Jul. 2015.

[4] S. Coogan, C. Flores, and P. Varaiya, "Traffic predictive control from low-rank structure," *Transp. Res. B, Methodol.,* vol. 97, pp. 1–22, Mar. 2017

[5] A. G. Sims, "The Sydney coordinated adaptive traffic system," in *Proc. Urban Transp. Division ASCE,* New York, 1979, pp. 12–27.

[6] P. B. Hunt, D. I. Robertson, R. D. Bretherton, and R. I. Winton, "SCOOT—A traffic responsive method for coordinating signals," in Transp. Road Res., Berkshire, U.K., Lab. Rep. no. LP 1014, 1981.

[7] J. J. Henry, J. L. Farges, and J. Tuffal, "The PRODYN real time traffic algorithm," in *Proc. 4th IFAC/IFIP/IFORS Conf. Control Transp. Syst.,* 1983, pp. 305–310.

[8] F. Boillot, S. Midenet, and J. C. Pierrelee, "The real-time urban traffic control system CRONOS: Algorithm and experiments," *Transp. Res. Part C: Emerging Technol.,* vol. 14, no. 1, pp. 18–38, Feb. 2006.

[9] F. Donati, V. Mauro, G. Roncoloni, et al, "A hierarchical decentralized traffic light control system-the first realisation: Progetto Torino". In *Proc. 9th IFAC World Congress,* Budapest, Hungary, 1984, pp. 2853–2858.

[10] N. H. Gartner, "OPAC: A demand-responsive strategy for traffic signal control," *Transp. Res. Rec.,* vol. 906, pp. 75–81, 1983.

[11] S. Sen and K. L. Head, "Controlled optimization of phases at an intersection," *Transp. Sci.,* vol. 31, no. 1, pp. 5–17, Feb. 1997.

[12] P. Mirchandani and L. Head, "A real-time traffic signal control system: Architecture, algorithm, and analysis," *Transp. Res. Part C: Emerging Technol.,* vol. 9, no. 6, pp. 415–432, Dec. 2001.

[13] SAE Int. DSRC Committee, "Dedicated short range communications (DSRC) message set dictionary," Soc. Automotive Eng., Warrendale, PA, USA, Tech. Rep. J2735_200911, Nov. 2009.

[14] C. Priemer and B. Friedrich, "A decentralized adaptive traffic signal control using V2I communication data," in *Proc. IEEE Conf. Intell. Transp. Syst.,* 2009, pp. 765–770

[15] L. Shen, R. Liu, Z. Yao, et al, "Development of dynamic platoon dispersion models for predictive traffic signal control," *IEEE Trans. Intell. Transp. Syst.*, vol. 20, no. 2, Feb. 2019.

[16] R. Ghaman, "Next-Generation smart traffic signals: RHODES(NG) with intellidrive(SM)—the self-taught traffic control system," Highway Traffic Control Systems, 2009.

[17] B. L. Smith, R. Venkatanarayana, H. Park, et al, "IntelliDrive traffic signal control algorithms," Center Transp. Studies, Univ. Virginia, Charlottesville, VA, USA, Tech. Rep. Final Report, 2010.

[18] N. J. Goodall, B. L. Smith, and B. B. Park, "Traffic signal control with connected vehicles," *J. Transp. Res. Board*, vol. 2381, no. 1, pp. 65–72, 2013.

[19] N. J. Goodall, "Traffic signal control with connected vehicles," Ph.D. Dissertation. University of Virginia, 2013.

[20] Q. He, K. Head, and J. Ding, "PAMSCOD: Platoon-based arterial multimodal signal control with online data," *Transp. Res. Part C, Emerg. Technol.*, vol. 20, no. 1, pp. 164–184, Feb. 2012.

[21] Q. He, K. L. Head, and J. Ding, "Multi-modal traffic signal control with priority, signal actuation and coordination," *Transp. Res. Part C, Emerg. Technol.*, vol. 46, pp. 65–82, Sep. 2014.

[22] D. McKenney and T. White, "Distributed and adaptive traffic signal control within a realistic traffic simulation," *Eng. Appl. Artif. Intell.*, vol. 26, no. 1, pp. 574–583, Jan. 2013.

[23] M. Ahmane, A. Abbas-Turki, F. Perronnet, et al, "Modeling and controlling an isolated urban intersection based on cooperative vehicles," *Transp. Res. C, Emerging Technol.*, vol. 28, pp. 44–62, Mar. 2013.

[24] J. Lee, B. Park, and I. Yun, "Cumulative travel-time responsive real-time intersection control algorithm in the connected vehicle environment," *J. Transp. Eng.*, vol. 139, no. 10, pp. 1020–1029, Oct. 2013.

[25] Y. Feng, K. L. Head, S. Khoshmagham, and M. Zamanipour, "A real-time adaptive signal control in a connected vehicle environment," *Transp. Res. C, Emerging Technol.*, vol. 55, pp. 460–473, 2015.

[26] C. Yan, H. Jiang, and S. Xie, "Capacity optimization of an isolated intersection under the phase swap sorting strategy," *Transp. Res., B, Methodol.*, vol. 60, pp. 85–106, Feb. 2014.

[27] C. Osorio, and K. Nanduri, "Urban transportation emissions mitigation: Coupling high-resolution vehicular emissions and traffic models for traffic signal optimization," *Transp. Res., B, Methodol.*, vol. 81, pp. 520-538, 2015.

[28] P. Li, P. Mirchandani, and X. Zhou, "Solving simultaneous route guidance and traffic signal optimization problem using space-phase-time hypernetwork," *Transp. Res., B, Methodol.*, vol. 81, pp. 103-130, 2015.

[29] K. Han, V. V. Gayah, B. Piccoli, et al, 2014. "On the continuum approximation of the on-and-off signal control on dynamic traffic networks," *Transp. Res., B, Methodol.*, vol. 61, pp. 73-97, 2014.

[30] D. W. Strong, M. R. Nagui, C. Ken, "New calculation method for existing and extended HCM delay estimation procedure," *in Proceedings of the 85th Annual Meeting*, Transportation Research Board, Washington, DC. 2006.

[31] A. PTV, "VISSIM 5.40 user manual," Karlsruhe, Germany, 2011.

[32] T. Tettamanti and I. Varga, "Development of road traffic control by using integrated VISSIM-MATLAB simulation environment," *Periodica Polytechn. Civil Eng.*, vol. 56, no. 1, pp. 43–49, 2012